SCAP is required for timely and proper myelin membrane synthesis

Mark H. G. Verheijen[a,1], Nutabi Camargo[a], Valerie Verdier[b], Karim Nadra[b], Anne-Sophie de Preux Charles[b], Jean-Jacques Médard[b], Adrienne Luoma[c], Michelle Crowther[c], Hideyo Inouye[c], Hitoshi Shimano[d], Su Chen[e], Jos F. Brouwers[f], J. Bernd Helms[f], M. Laura Feltri[g], Lawrence Wrabetz[g], Daniel Kirschner[c], Roman Chrast[b], and August. B. Smit[a]

[a]Department of Molecular and Cellular Neurobiology, Center for Neurogenomics and Cognitive Research, Neuroscience Campus Amsterdam, VU University, 1081 HV, Amsterdam, The Netherlands; [b]Department of Medical Genetics, University of Lausanne, CH-1005 Lausanne, Switzerland; [c]Biology Department, Boston College, Chestnut Hill, MA 02467; [d]Department of Internal Medicine (Endocrinology and Metabolism), Graduate School of Comprehensive Human Sciences, University of Tsukuba, Ibaraki 305-8577, Japan; [e]Chainon Neurotrophin Biotechnology Inc., Malta, NY 12020; [f]Department of Biochemistry and Cell Biology, Faculty of Veterinary Medicine, Utrecht University, 3508 TC, Utrecht, The Netherlands; and [g]San Raffaele Scientific Institute, Division of Genetics and Cell Biology, Milan, Italy

Edited by James L. Salzer, NYU School of Medicine, New York, NY, and accepted by the Editorial Board October 20, 2009 (received for review May 22, 2009)

Myelination requires a massive increase in glial cell membrane synthesis. Here, we demonstrate that the acute phase of myelin lipid synthesis is regulated by sterol regulatory element-binding protein (SREBP) cleavage activation protein (SCAP), an activator of SREBPs. Deletion of SCAP in Schwann cells led to a loss of SREBP-mediated gene expression involving cholesterol and fatty acid synthesis. Schwann cell SCAP mutant mice show congenital hypomyelination and abnormal gait. Interestingly, aging SCAP mutant mice showed partial regain of function; they exhibited improved gait and produced small amounts of myelin indicating a slow SCAP-independent uptake of external lipids. Accordingly, extracellular lipoproteins partially rescued myelination by SCAP mutant Schwann cells. However, SCAP mutant myelin never reached normal thickness and had biophysical abnormalities concordant with abnormal lipid composition. These data demonstrate that SCAP-mediated regulation of glial lipogenesis is key to the proper synthesis of myelin membrane, and provide insight into abnormal Schwann cell function under conditions affecting lipid metabolism.

lipid metabolism | neuron-glia interactions | neuropathy | X-ray diffraction

The rapid saltatory conduction of neuronal action potentials is crucially dependent on the insulating myelin membrane, an organelle synthesized by Schwann cells in the PNS, and by oligodendrocytes in the CNS (1). The electrical insulating property of the myelin membrane is provided by its high and characteristic lipid content with high levels of cholesterol, galactosphingolipids, and saturated long-chain fatty acids (1). Accordingly, metabolic disorders of cholesterol [e.g., Smith-Lemli-Opitz-syndrome and Tangier disease (2, 3)], galactosphingolipids (4, 5), or of fatty acid metabolism [Refsum's disease and diabetes mellitus (2)] often produce myelin defects.

With the Schwann cell membrane surface area expanding a spectacular 6,500-fold during myelination (6), it is obvious that production of myelin membrane requires a large amount and diversity of myelin proteins and lipids. Myelination of peripheral nerves is a highly dynamic process with an acute phase that peaks in the second postnatal week in the mouse and a phase of steady-state maintenance in adult nerves (7). While it has been suggested that many of the myelin lipids are synthesized in the nerve itself, as was demonstrated for cholesterol (8, 9), the factors regulating their synthesis in myelinating Schwann cells are largely unknown. We recently profiled transcription in the peripheral nerve during myelination and found that sterol regulatory element-binding proteins (SREBPs) are highly expressed in myelinating Schwann cells (10–12). SREBPs, consisting of SREBP-1a, SREBP-1c, and SREBP-2, belong to the family of basic helix–loop–helix-leucine zipper (bHLH-Zip) transcription factors that regulate lipid metabolism. SREBP-1c and SREBP-2 preferentially govern the transcriptional activation of genes involved in fatty acid and cholesterol metabolism, respectively, whereas SREBP-1a activates both pathways (13). SREBP transcription factors crucially rely on post-translational activation involving the sterol sensor SCAP. When sterol levels are low, SCAP escorts the SREBPs from the ER to the Golgi, where they are activated by processing through the membrane-associated proteases, S1P and S2P. The resulting mature and transcriptionally active forms of the SREBPs translocate to the nucleus where they bind genes containing sterol regulatory elements (13, 14).

Here, we determined the role of SCAP in myelination by its conditional ablation in Schwann cells. We found that deletion of SCAP seriously affected the dynamics of myelin membrane synthesis and caused neuropathy. However, these phenotypes improved with aging; SCAP mutant Schwann cells were able to slowly synthesize myelin, in an external lipid-dependent fashion, resulting in myelin membrane defects that are associated with abnormal lipid composition. Our data demonstrated the crucial role of SCAP-mediated control of cholesterol and lipid metabolism necessary for production of a proper myelin membrane by Schwann cells.

Results

SCAP Deletion Interferes with the Acute Phase of Myelination. We generated mice carrying a Schwann cell-specific deletion of the SCAP gene by crossing mice in which the promoter and the first exon of the SCAP gene is flanked by loxP sites (SCAPloxP/loxP mice) (14), with mice expressing Cre recombinase specifically in Schwann cells starting at E14 (P0-Cre) (15) (Fig. S1*A*). We detected Cre-mediated recombination of the SCAP gene in the sciatic nerve endoneurium from E17 onwards, which was absent in the perineurium/epineurium of the same nerve samples (Fig. S1*B*). Schwann cells constitute a large majority of the cells present in the endoneurium of the peripheral nerve (16). In line with this, both SCAP mRNA (Fig. S2*A*) and protein levels (Fig. S2*B*) were strongly reduced in mutant sciatic nerve endoneurium. The PCR detectable nonrecombined SCAP gene and concomitant residual SCAP expression in the endoneurium of the conditional mutant mice is from other endoneurial cell types lacking the P0-driven Cre (15). Schwann cell-specific SCAP mutant mice were born with normal Mendelian ratios and could be distinguished from their

Author contributions: M.H.G.V. and R.C. designed research; M.H.G.V., N.C., V.V., K.N., A.-S.d.P.C., J.-J.M., A.L., M.C., H.I., J.F.B., L.W., and D.K. performed research; M.H.G.V., H.S., and M.L.F. contributed new reagents/analytic tools; M.H.G.V., N.C., V.V., K.N., A.-S.d.P.C., A.L., H.I., S.C., J.F.B., L.W., and D.K. analyzed data; and M.H.G.V., J.B.H., M.L.F., D.K., R.C., and A.B.S. wrote the paper.

The authors declare no conflict of interest.

This article is a PNAS Direct Submission. J.L.S. is a guest editor invited by the Editorial Board.

[1]To whom correspondence should be addressed. E-mail: mark.verheijen@cncr.vu.nl.

This article contains supporting information online at www.pnas.org/cgi/content/full/0905633106/DCSupplemental.

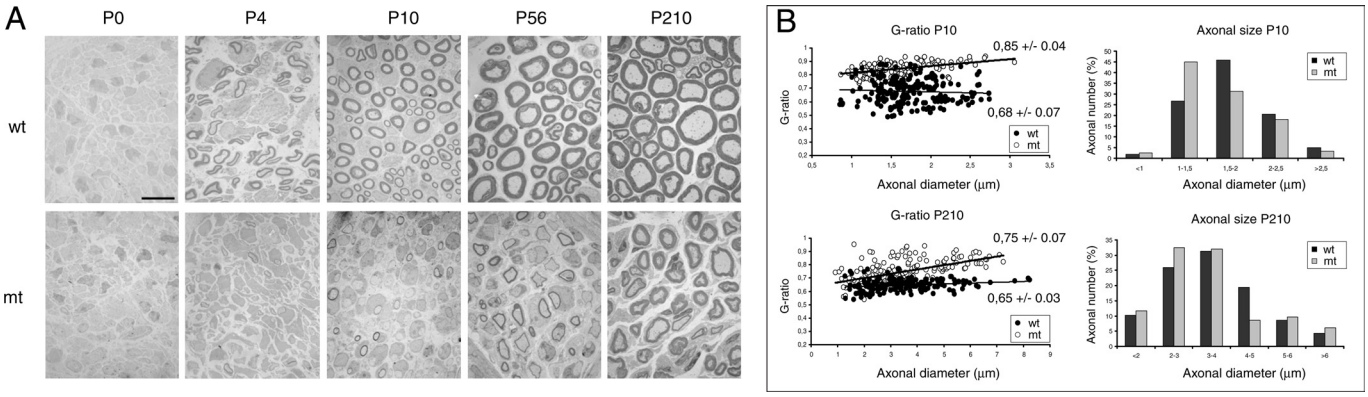

Fig. 1. SCAP mutant nerves are defective in the acute phase of myelination. (*A*) Electron microscopic analysis of sciatic nerve myelination in cross-sections of either wild-type (wt) or mutant (mt) mice at depicted time points. (Scale bar, 10 μm.) (*B*) Morphometric analysis of myelinated axons on sciatic nerves of mutant and wild-type mice, showing g-ratio (axon diameter: myelinated fiber diameter) and axonal size distribution at P10 and P210.

wild-type littermates by a general tremor and unsteady gait after postnatal week 3. The unsteady gait persisted into early adulthood, and surprisingly, became less apparent in older adults (Movie S1–S4). Improvement of this typical neuropathy-related behavior never reached completeness, as also shown by the abnormal reaction of mutant mice when tail-lifted (Fig. S2*C*).

Electron microscopy (EM) of sciatic nerves (Fig. 1*A*) showed that in the control nerve, myelination started at P4, was fully ongoing at P10 and completed in adult nerves (P56–P210). By contrast, mutant nerves were virtually devoid of myelin at P4–P10, and were severely hypomyelinated in adults. However, some thin myelin was formed which increased with aging (P56 vs. P210). The percentage of axons that were myelinated was normalized at P210 (Fig. S3*A*). Myelination of the optic nerve was normal, which is in line with the optic nerve being myelinated by SCAP-expressing oligodendrocytes (Fig. S3*B*). G-ratio measurements, indicating the ratio of axon diameter versus myelinated fiber diameter, confirmed that hypomyelination of the sciatic nerve was severe at P10 and still present, although less pronounced, at P210 (Fig. 1*B*). Remarkably, axon diameter distribution was affected as well, at both P10 and P210, with a shift of medium-large diameter axons to smaller axons. Also, EM analysis of mutant nerves showed proper 1:1 relationship with large caliber axons at P0 (promyelination, Fig. 2*A*). However, most mutant Schwann cells were retained in this promyelination stage at P4 (Fig. 2 *B* and *C*, mt and wt, respectively) and P10 (Fig. 2*D*), but their number was at almost normal levels at P210 (Fig. 2, graph). Accordingly, P56 mutant nerves contained more Schwann cells and had prolonged expression of immature Schwann cell markers (Oct-6/SCIP, NgfR and cyclinD1), while their expression reduced with aging (P56 vs. P210, Fig. S4). Adult mutant nerves showed basal lamina onion bulb formation, increased collagen deposition (Fig. 2*E*), but no signs of inflammation. Mutant adult-stage non-myelinated fibers showed no structural Schwann cell abnormalities and the number of axons per bundle was not significantly different (Fig. S5).

Taken together, analysis of the SCAP mutant mice showed that mutant Schwann cells were mostly affected in the developmentally regulated synthesis of myelin, and slowly produced myelin at later developmental stages leading to improvement in peripheral neuropathy-associated behavior.

SCAP Deletion Causes a Loss of SREBP-Mediated Gene Expression. SCAP is specifically required for processing of SREBPs into active transcription factors (14). We therefore determined the effect of SCAP deletion on SREBP-directed gene expression in sciatic endoneurium from P0 until P210 (Fig. 3). First, SCAP mRNA levels increased during postnatal development in normal nerves, while they were continuously low in mutant nerves. Second, transcript levels for all three SREBP isoforms were high during myelination in normal nerves and subsequently modestly down-regulated after myelination. SREBP1c mRNA level remained relatively high long after the process of myelination was completed,

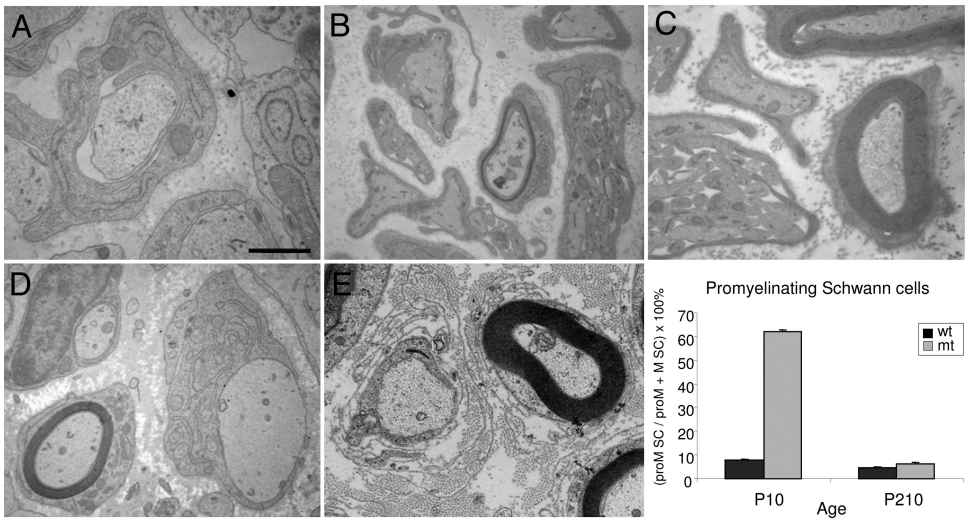

Fig. 2. Ultrastructural analysis of congenital hypomyelination in SCAP mutant nerves. Electron micrographs of wild-type and SCAP mutant sciatic nerves showing (*A*) normal promyelin figure in mutant at P0, (*B*) thinner myelin and lower number of myelinated axons in mutant at P4, compared to wild-type at P4 (*C*). (*D*) Some axons are becoming myelinated in mutant at P10, while others do not. (*E*) Myelinated and promyelinated fibers in mutant nerves (P56) show basal lamina onion bulbs and increased extracellular collagen. [Scale bar, (*A*) 0.5 μm; (*B* and *C*) 1 μm, (*D*) 1.67 μm; and (*E*) 1.26 μm.] Graph shows number of Schwann cells in promyelin stage as a percentage of the total number of promyelin and myelinating Schwann cells, for wild-type (wt) and mutant (mt), at postnatal ages P10 and P210. The data represent the mean ± standard deviation of triplicate measurements.

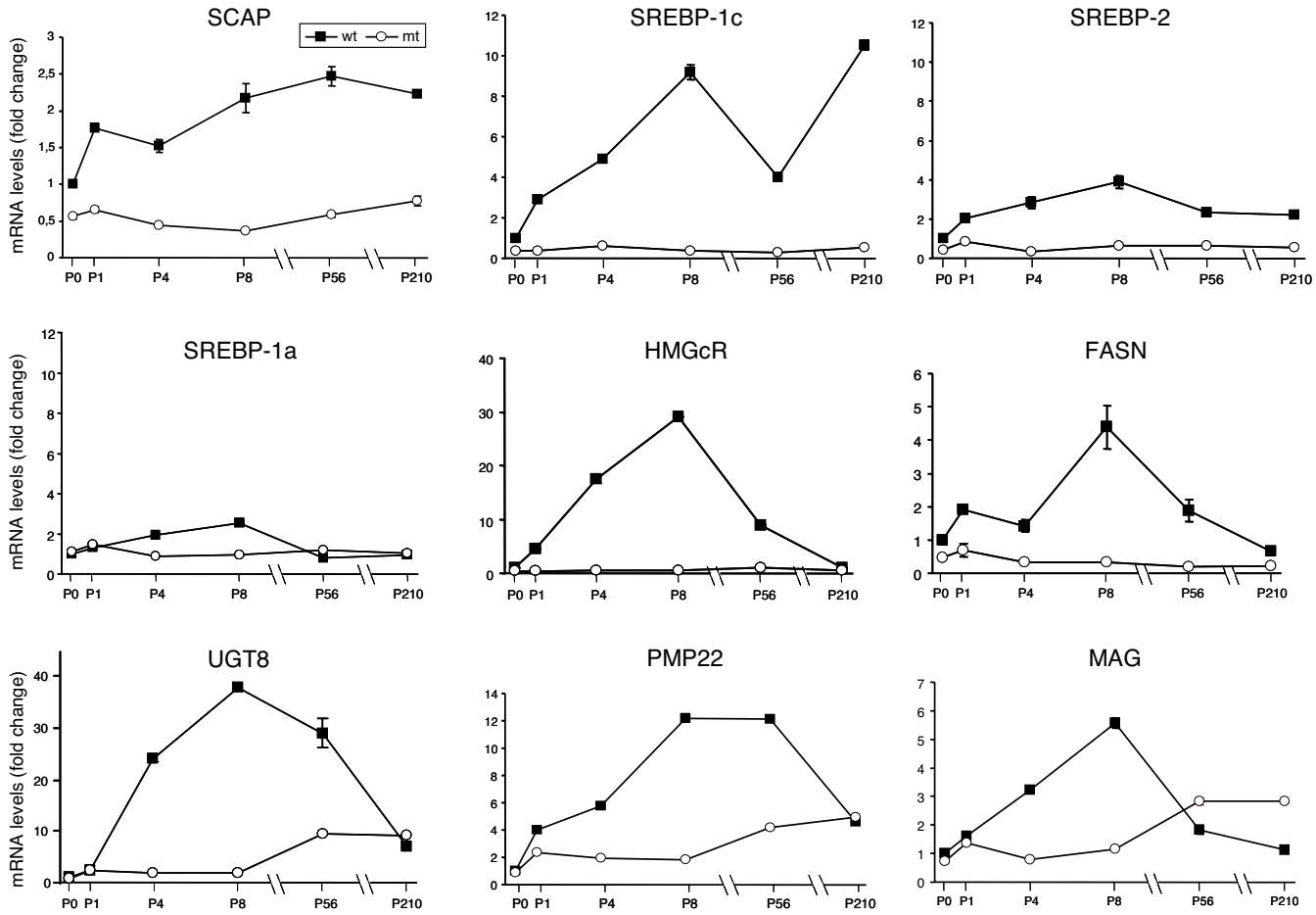

Fig. 3. Deletion of SCAP in Schwann cells prevents SREBPs-mediated gene expression and reduces structural myelin gene expression. Quantitative PCR analysis of mRNA levels for depicted genes of wild-type (wt) or SCAP mutant (mt) animals in total sciatic nerves (P0, P1, P4, and P8) or sciatic nerve endoneurium (P56 and P210). SREBP1c mRNA level remained relatively high long after the process of myelination was completed, as reported by us in ref. 12. SREBP2 and SREBP1c are the predominantly expressed forms in the endoneurium, whereas expression of SREBP1a is very low (12). Expression level at time point P0 in wild-type sample was arbitrarily set to 1 and level in mutant sample was accordingly normalized. For all other time points, the mRNA levels are represented as fold increase over the mRNA expression level at P0. The data represent the mean ± standard deviation of triplicate measurements.

as reported by us in ref. 12. In mutant endoneurium transcript levels of SREBP2 and SREBP1c, and to a lesser extent SREBP1a, were low and stayed low during aging. Residual SCAP and SREBP transcripts in mutant endoneurium were likely derived from non-Schwann cells. Third, mRNA levels of HMGcR and FASN, the rate-limiting enzymes in cholesterol and fatty acid synthesis, respectively, and under control of SREBPs, were maximally increased during myelination in normal nerves as reported in ref. 10, whereas they were very low in mutant nerves. Interestingly, mRNA levels of UGT8, the rate–limiting enzyme for myelin galactolipid synthesis (4, 5) was also reduced in mutant nerves but unlike the SREBP target genes (e.g., FASN and HMGcR), it followed the expression of myelin protein genes, which in mutant nerves lacks the peak in the second postnatal week that was found during myelination in normal nerves, but instead slowly increased during aging (Fig. 3). Taken together, we conclude that deletion of SCAP in Schwann cells abolishes dynamic expression of SREBPs and their target genes involved in lipid metabolism, and that indeed SCAP regulates, via the activation of SREBPs, the expression of the SREBP genes (14). Consistent with this model, we found that siRNA-mediated knock down of SCAP in primary cultured Schwann cells in vitro caused lower SREBP protein and mRNA levels, as well as decreased transcript levels of the SREBP target gene SCD1 (Fig. S6 *A* and *B*), and also that active forms of SREBP-1c or SREBP-1a induced SREBP-1c promoter activity in Schwann cells (Fig. S6*C*).

Myelination by SCAP Mutant Schwann Cells Is Dependent on Extracellular Lipids. Despite the very low levels of lipogenic transcripts that we detected in the endoneurium, SCAP mutant Schwann cells are still able to produce some myelin. To determine whether the uptake of lipids may underlie the synthesis of myelin membrane by SCAP mutant Schwann cells, we cultured DRG explants of wild-type and SCAP mutant mice under different lipid conditions. First, myelination by mutant DRGs was less successful compared to that of wild-type DRGs, and thus consistent with the observed differences in vivo (Fig. 4). Second, myelination by SCAP mutant Schwann cells of DRG neurons was completely prevented in lipoprotein-deficient medium, and was rescued by addition of lipoproteins. Notably, also myelination of wild-type DRG neurons was strongly reduced under lipoprotein-free conditions, and stimulated by the addition of lipoproteins, a finding similar to recent observations by Saher et al. (9) who showed that extracellular cholesterol accelerates myelination in vitro. Because myelination by SCAP mutant Schwann cells in vitro is fully dependent on extracellular lipids, it is very likely that SCAP mutant Schwann cells are dependent on SCAP-SREBP-independent lipid uptake in vivo.

SCAP Mutant Myelin Membrane Has Biophysical Abnormalities Related to Abnormal Lipid Composition. Lipid profiling of purified myelin (P210) revealed minor changes in lipid classes, when normalized to phosphatidyl choline, reduced levels in mutant myelin

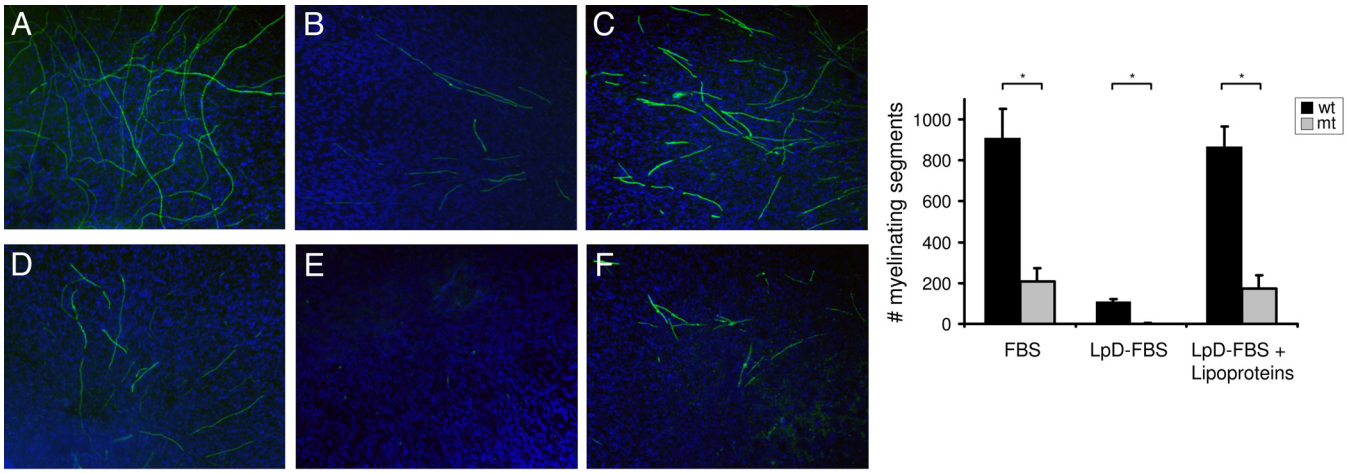

Fig. 4. Myelination by SCAP mutant Schwann cells is fully dependent on extracellular lipids. DRG explants of wild-type (*A–C*) or SCAP mutant mice (*D–F*) were cultured for 19 days in medium containing ascorbic acid to induce myelination and with FBS (*A* and *D*), lipoprotein-deficient FBS (LpD-FBS) (*B* and *E*), or LpD-FBS with lipoproteins (LpD-FBS + Lp) (*C* and *F*). The level of myelination was evaluated by immunohistological staining with an Mpz antibody (green). Cell nuclei were stained with DAPI (blue). (Graph) The number of myelinated segments in wild-type (wt) or SCAP mutant (mt) DRGs cultured under the conditions described in *A–F* was counted. The data represent the mean ± standard error of the mean of at least triplicate samples. (*) All *P* values are <0.01.

were found for phosphatidyl serine (to 85% of control levels), sulfatides (85%), and cholesterol (80%), whereas levels of the major lipids phosphatidyl ethanolamine and glycosphingolipids were not changed (Fig. 5*A*). We next investigated the fatty acid composition of phospholipids and found a significant shift in the level of monounsaturated fatty acids toward polyunsaturated fatty acids, and a decrease in the ratio of 18:1/18:2 in mutant nerves (Fig. 5*A* and Fig. S7*A*). Lipid fingerprinting of intact phospholipids from six mutant and six wild-type nerves and analysis using principal component analysis (PCA) showed that most of the variance in phospholipid species between samples was accounted for by differences between mutant and wild-type nerves (Fig. S7*B*), and identified several lipid species that significantly contribute to these differences (Fig. 5*B* and Fig. S7*C*). In line with the increase in polyunsaturated fatty acids in the mutant nerves, the mutant-specific phospholipid species were more unsaturated compared to the wild-type specific species.

To determine whether the abnormal lipid content may relate to structural myelin membrane abnormalities, we performed EM analysis of myelin membranes of SCAP mutant Schwann cells. This analysis did not reveal any major abnormalities in packing and periodicity of myelin membrane layers at either an early developmental stage (P4, Fig. S8*A*) nor in mature nerves (P56, periodicity of mutant vs. wt: 131.7 ± 2.8 Å vs. 132.2 ± 1.6 Å). To accurately measure myelin period and membrane packing, we analyzed the internodal myelin of unfixed late adult mutants by using X-ray diffraction (XRD) (17, 18). The relative amount of mutant myelin in sciatic nerve was close to one-half (0.57) of wild-type myelin at P210, due to a reduction in average myelin sheath thickness, whereas no differences were found for the optic nerve (Fig. 5*C*). Consistent with EM, XRD showed that the myelin period (d) in sciatic nerve was virtually indistinguishable between mutant and wild-type (respectively, 176.1 ± 0.8 Å versus 176.5 ± 0.6 Å). However, the width of the cytoplasmic space (cyt) between two membrane bilayers was significantly smaller, and the width of the extracellular apposition (ext) was significantly larger (Fig. 5*D*). No differences were found in the thickness of the membrane bilayer (lpg). Next, to determine whether the abnormalities found in mutant myelin may correlate with the abnormal lipid content of the mutant endoneurium, we used a point-focus X-ray beam to examine the wide-angle scatter from the fatty acyl chains in the internodal myelin. Both wild-type and mutant showed well-oriented, wide-angle scatter from the fatty acyl chains, with the mutant nerve giving weaker scatter than the wild-type nerve (Fig. 5*E*), which was consistent with the observed hypomyelination in the mutant mice. The observed spacings for the fatty acyl ring, a measurement for the lateral packing of fatty acyl chains (19), and the integral width of the fatty acyl ring in the radial direction, a measurement of the short range order and crystallinity of fatty acyl chains (20, 21), were similar between wild-type and SCAP mutant nerves for both sciatic and optic nerve (Fig. 5*F* and Fig. S8 *B* and *C*). Interestingly, the integral arc-width (integral-width spread along the circumference of the fatty acyl ring), which reflects the level of fatty acyl disordering (19), was significantly larger for the SCAP mutant than for the wild-type in sciatic nerve (Fig. 5*F* and Fig. S8*C*) These data suggest that the peripheral myelin membrane that is slowly being synthesized in mutant animals contains disordered lipid bilayers, as a consequence of abnormal lipid content, which may underlie the observed fine-structural abnormalities in the SCAP mutant myelin membrane.

Discussion

SCAP Deletion in Schwann Cells Causes Congenital Hypomyelination. We showed that SCAP is required for activation of SREBP-mediated transcription in myelinating Schwann cells, and observed that SCAP mutant peripheral nerves are essentially devoid of myelin in the first postnatal weeks and very slowly build up some myelin membrane with age. The number of promyelinating Schwann cells was increased in the first weeks after birth, but returned to normal with aging, suggesting that Schwann cell differentiation is not arrested, but is delayed. Together with the observed peripheral neuropathy of mutant mice, this phenotype is characteristic for congenital hypomyelination (2). Also, the basal lamina onion bulbs that we found in mutant nerves, indicative of layers that have been left behind by the withdrawal of Schwann cell processes, are commonly observed in congenital hypomyelinating neuropathy (22).

Abnormal Myelin Synthesis by Adult SCAP Mutant Schwann Cells. An interesting finding of our study is that despite the strong decrease in expression of enzymes involved in cholesterol and fatty acid synthesis, SCAP mutant peripheral nerves are able to produce some myelin. At first sight, this myelin may result from residual enzymatic activities in mutant Schwann cells. However, mutant nerves contain more polyunsaturated fatty acids and different phospholipid species are present in mutant nerves, suggesting that

A

Lipid	wt	mt
Phosphatidyl ethanolamine	124,4 ± 21,6	107,9 ± 20,5
Phosphatidyl inositol	7,5 ± 1,4	6,8 ± 1,1
Phosphatidyl serine	64,9 ± 7,8	55, ± 8,6*
Sphingomyelin	57,0 ± 3,9	64,6 ± 3,1**
Glycosphingolipids	136,9 ± 22,0	122,9 ± 11,7
Sulfatides	65,3 ± 9,5	54,9 ± 8,6*
Cholesterol	449,0 ± 27,9	356,5 ± 22,1**
Saturated FA (%)	43,1 ± 1,1	46,8 ± 4,5
Monounsaturated FA (%)	44,6 ± 1,5	37,0 ± 3,3***
Polyunsaturated FA (%)	12,3 ± 1,5	16,2 ± 1,5***
C18:1/C18:2	12,4 ± 2,7	5,9 ± 0,7***

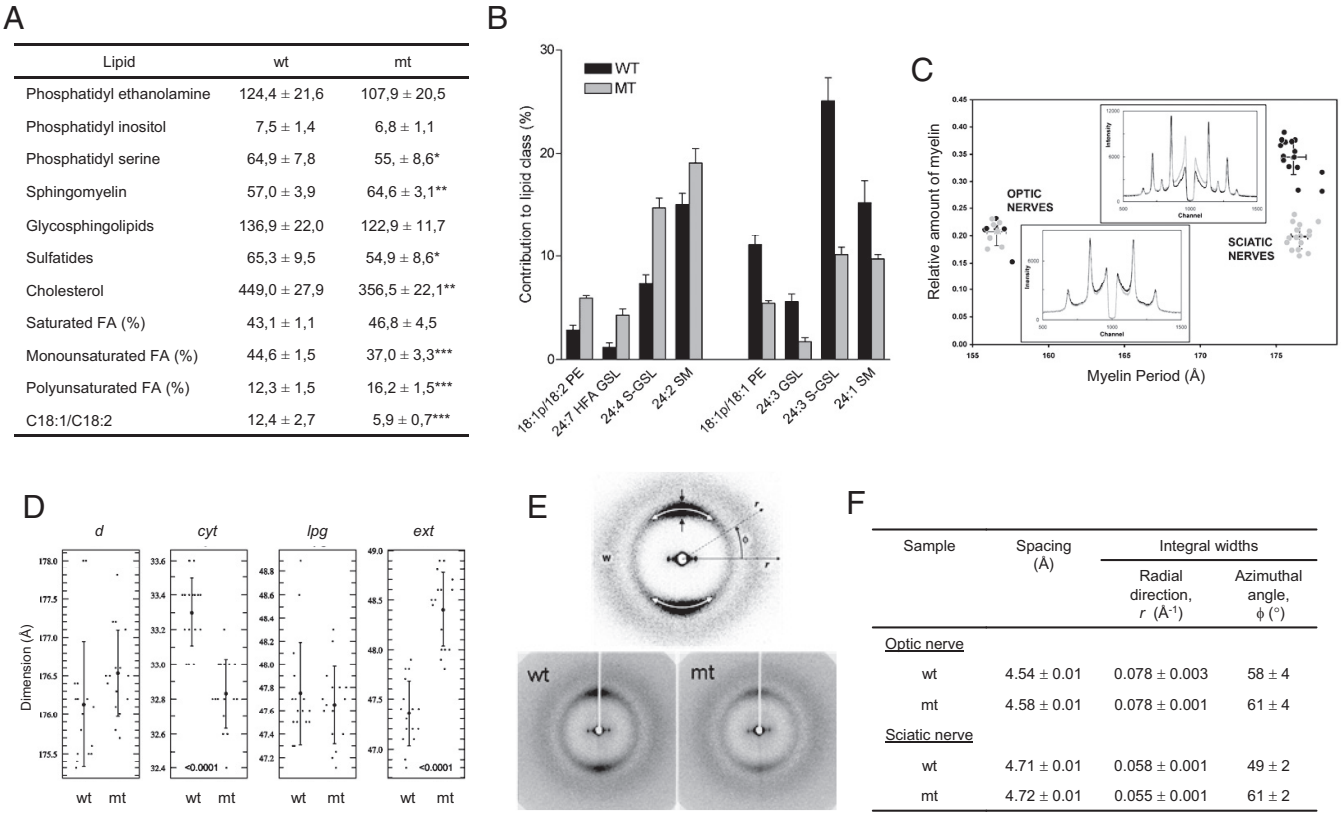

F

Sample	Spacing (Å)	Integral widths	
		Radial direction, r (Å^{-1})	Azimuthal angle, ϕ (°)
Optic nerve			
wt	4.54 ± 0.01	0.078 ± 0.003	58 ± 4
mt	4.58 ± 0.01	0.078 ± 0.001	61 ± 4
Sciatic nerve			
wt	4.71 ± 0.01	0.058 ± 0.001	49 ± 2
mt	4.72 ± 0.01	0.055 ± 0.001	61 ± 2

Fig. 5. Adult SCAP-mutant myelin contains fine structural defects associated with altered lipid profile. (*A*) Lipid extracts of purified myelin of sciatic nerve of P210 wild-type or SCAP mutant mice were analyzed by using mass spectrometry. Depicted are the amounts of lipid species normalized to phosphatidyl choline, the percentage of polyunsaturated, monounsaturated or saturated fatty acids and the ratio of 18:1/18:2 based on the measurements shown in Fig. S7*A*. *, $P < 0.05$; **, $P < 0.01$; ***, $P < 0.001$. (*B*) Shown is a selection of phospholipids that are most significantly different between lipid extracts of purified myelin of P210 wild-type versus SCAP mutant mice, as determined with principle component analysis as shown in Fig. S7 *B* and *C*. The data represent the mean ± standard deviation of measurements on six nerves per genotype. PE, phosphatidyl ethanolamine; SM, sphingomyelin; GSL, glycosphingolipid; S-GSL, Sulfatide GSL; and HFA GSL, alpha-hydroxy-fatty acid GSL. All *P* values <0.001. (*C*) XRD analysis of myelin of wild-type (black) and SCAP mutant (gray) at P210 of sciatic nerve and optic nerve. Shown is the relation between myelin period (in Ångstrom) and relative amount of myelin [M/(M+B), see *Materials and Methods*]. (*D*) XRD analysis of myelin of wild-type (wt) and SCAP mutant (mt) sciatic nerves at P210 shows myelin period (*d*), thickness of the lipid bilayer (lpg), width of the cytoplasmic space (cyt) between two membrane bilayers and the width of the extracellular apposition (ext). (*E*) Point-focus XRD analysis of myelin of wild-type and SCAP mutant sciatic nerves at P210. Shown in the explanation figure (*E*, *Upper*) are the well-oriented wide-angle scatter from the fatty acyl chains (white arrows) and scatter from H_2O molecules (*W*). Quantifications are summarized in *F*. The observed spacing for the fatty acyl ring is a measurement of the lateral packing of fatty acyl chains. The integral width of the fatty acyl ring in the radial direction (between black arrows) is a measurement of the short range order and crystallinity of fatty acyl chains. The integral arc-width (length of the white arrows in the fatty acyl ring) reflects the level of fatty acyl disordering.

these fatty acids may not be synthesized nor fully metabolized in the Schwann cells but instead are partially derived from an extracellular source. Our observation that extracellular cholesterol and phospholipids, when bound to lipoproteins, rescue the block of myelination in SCAP mutant DRG explants cultured under lipid-free conditions is consistent with this. The source of extracellular-derived lipids is unclear, but may involve other cells in the endoneurium and/or the circulation. Saher et al. (3) showed that mice carrying an oligodendrocyte-specific deletion of squalene synthase (SQS), which is required for cholesterol synthesis, have CNS hypomyelination that becomes close to normal after 3 months, and they suggested that horizontal cholesterol transfer from neighboring astrocytes to cholesterol-deficient oligodendrocytes, via lipoprotein receptor dependent uptake, might underlie this. Similarly, SCAP mutant Schwann cells may take up cholesterol derived from other cells in the endoneurium. Data of Jurevics and Morell indicated that a small fraction (15%) of cholesterol in adult PNS myelin is derived from outside the endoneurium (8), although injury-induced disruption of the bloodnerve barrier did not cause more utilization of circulating cholesterol (23). We observe in SCAP mutant mice (in which both cholesterol and fatty acid biosynthesis are affected) that myelin contains more polyunsaturated fatty acids, and have higher C18:2 levels, which is consistent with an increased uptake of essential fatty acids from external sources (7). Consistent with this, others have demonstrated that circulating fatty acids are slowly incorporated in adult myelin (24, 25). Therefore, in the situation of local hypolipidemia induced by SCAP inactivation, Schwann cells may use fatty acids derived from the circulation or from other nerve compartments, such as the perineurium or epineurium, as suggested in ref. 10. Taken together, compromised Schwann cell SREBP activation, as in our SCAP mutant, leads to a slow rate of myelin synthesis that is likely dependent on the uptake of lipids.

By using X-ray diffraction, we found that SCAP mutant myelin membrane had a wider extracellular apposition while showing decreased cytoplasmic separation between membrane bilayers together with increased disordering of fatty acids. Thus, the fatty acids, derived via uptake from extracellular sources or abnormal lipid metabolism, have a decreased level of fatty acid saturation, which together with the different phospholipid species may lead to different lipid-protein interactions causing the altered packing of proteins in the membrane (26) and consequent myelin abnormalities.

Implications for Disorders of Lipid Metabolism Associated with Neuropathy. Our study may provide insight into neuropathies that are associated with defective lipid metabolism in myelinating glia (2). Abnormal fatty acid metabolism was previously proposed as one of the contributing factors in the pathogenesis of diabetic peripheral neuropathy (DPN) (27), including a lower phospholipid 18:1 to 18:2 ratio in the nerve (28). We recently showed that Schwann cell SREBP-1c mediated fatty acid metabolism is down-regulated in diabetic rat and mice and we proposed that this might underlie the DPN observed in these animals (11, 12). Our current observations that compromised Schwann cell SREBP activation interferes with myelination and myelin lipid composition, is in line with an important role of Schwann cell fatty acid metabolism in the pathophysiology of DPN.

In conclusion, we identified the SCAP-SREBP pathway governing the massive lipid synthesis by Schwann cells that is required for myelin membrane expansion. Our data show the myelin membrane defects that are a consequence of attenuated endogenous lipid synthesis. Our findings provide important functional insight into the regulation and role of endogenous Schwann cell lipid metabolism in myelination and may have important implications for the understanding of neuropathies associated with lipid metabolic disorders, such as diabetes mellitus.

Materials and Methods

Mice. SCAP-floxed mice (hereafter SCAPloxP/loxP mice) were from the Jackson Laboratory and have been described in ref. 14. mP0TOTA(Cre) mice (hereafter P0cre) have been described (15). Both of these mouse lines were maintained on a C57Bl6 background. Throughout the text, mice of the P0cre/SCAPloxP/loxP genotype were referred to as 'SCAP mutant mice,' mice of SCAPloxP/loxP genotype were referred to as 'wild-type mice.' All primer sequences are in Table S1 .

XRD Analysis. Sciatic and optic nerves were dissected from P210 wild-type and SCAP mutant animals and sealed in capillary tubes as described in ref. 17. For XRD analysis of internodal myelin lamellar structure, the capillary was mounted on a single-mirror, Franks-camera set-up on a 3.0 kW Rigaku X-ray generator. Thirty-minute X-ray exposures were recorded using a linear, position-sensitive detector. Measurement of the positions of the reflections gave the periodicity of myelin from Bragg's law, and quantitation of the intensities above background [M/(M+B), with M = total integrated intensity, and B = background intensity]. See ref. 17 for further details. For XRD analysis of parameters relating to the fatty acyl chains, 2-D, wide-angle patterns were measured by using the point-focus, CuKα X-ray beam generated by the Oxford diffraction Xcalibur PX Ultra system located in the laboratory of Andrew Bohm (Department of Biochemistry, Tufts University, Boston, MA). The detector was an Onyx CCD, and the sample-to-detector distance was calibrated as above. Exposure time was 150 s for each sample. See Inouye et al. (20) for further details.

Lipid Analysis. Sciatic nerves from P210 animals were isolated, the endoneurium was isolated, used for myelin purification by density gradient centrifugation (29), and lipids were isolated by using a chloroform:methanol mixture (2:1, vol/vol). Neutral lipids were analyzed on a Sciex 4000QTRAP mass spectrometer, equipped with an atmospheric pressure chemical ionization (APCI) source. Before infusion, neutral lipids were separated on a Lichrospher RP18e column by using a gradient from acetonitrile to acetone. Phospholipids, glycosphingolipids, and free fatty acids obtained by hydrolysis of phospholipids were analyzed as described (30, 31) by using defined molecular species and authentic free fatty acid standards as standards for quantification purposes.

DRG Explant Cultures. Dorsal root ganglia were dissected from wild-type and SCAP mutant mice at embryonic day 14 (E14), as described in ref. 32. Isolated DRGs were grown individually on coverslips coated with polyL-lysine and laminin in C-medium (32). After 5 days, myelination was induced by culturing the DRG explants in C-medium, supplemented with 50 μg/mL ascorbic acid, and with or without FBS (10%), lipoprotein-deficient (LpD)-FBS (10%, from Sigma) or LpD-FBS (10%) + bovine lipoproteins (750 ng/mL). The media with fresh NGF and ascorbic acid were changed every 2–3 days. Explants were harvested after 19 days in culture. The number of myelinated segments was determined after staining with an antibody recognizing P0 glycoprotein (P07).

Additional Methods. Description of additional methods, including microdissection of sciatic nerve, quantitative PCR, electron microscopy, and morphometric analysis, cell culture, transfections, luciferase assays, and Western blot analysis are available in the *SI Text*.

ACKNOWLEDGMENTS. We thank William Hendriks for assistance with animal techniques, Carry Moorer-van Delft and Jan van Minnen for assistance with electron microscopy, and Dr. J. J. Archelos for generous supply of anti-Mpz antibody. M.L.F. and L.W. thank Desiree Zambroni for expert technical assistance. This work was supported by the Dutch Brain Foundation Grant 13F05.50 (to M.H.G.V.), European Union Grant EU-NEST 12702 (to M.H.G.V.), Centre for Medical Systems Biology (A.B.S), Marie Curie Foundation Host Fellowship EST-2005–020919 (to N.C.), Swiss National Science Foundation Grant PP00A-106714 (to R.C.), the National Institutes of Health Grants R01 NS045630 (to M.L.F.) and R01 NS055256 (to L.W.) and Telethon Italia Grants GGP08021 (to M.L.F.) and GGP071100 (to L.W.).

1. Garbay B, Heape AM, Sargueil F, Cassagne C (2000) Myelin synthesis in the peripheral nervous system. *Prog Neurobiol* 613:267–304.
2. Dyck PJ, Thomas PK (2005) Peripheral Neuropathy (Elsevier Saunders, Philadelphia, PA), 4th Ed.
3. Saher G, et al. (2005) High cholesterol level is essential for myelin membrane growth. *Nat Neurosci* 84:468–475.
4. Coetzee T, et al. (1996) Myelination in the absence of galactocerebroside and sulfatide: Normal structure with abnormal function and regional instability. *Cell* 862:209–219.
5. Bosio A, Binczek E, Stoffel W (1996) Functional breakdown of the lipid bilayer of the myelin membrane in central and peripheral nervous system by disrupted galactocerebroside synthesis. *Proc Natl Acad Sci USA* 9323:13280–13285.
6. Webster HD (1971) The geometry of peripheral myelin sheaths during their formation and growth in rat sciatic nerves. *J Cell Biol* 482:348–367.
7. Garbay B, et al. (1998) Regulation of oleoyl-CoA synthesis in the peripheral nervous system: Demonstration of a link with myelin synthesis. *J Neurochem* 714:1719–1726.
8. Jurevics HA, Morell P (1994) Sources of cholesterol for kidney and nerve during development. *J Lipid Res* 351:112–120.
9. Saher G, et al. (2009) Cholesterol regulates the endoplasmic reticulum exit of the major membrane protein P0 required for peripheral myelin compaction. *J Neurosci* 2919:6094–6104.
10. Verheijen MH, Chrast R, Burrola P, Lemke G (2003) Local regulation of fat metabolism in peripheral nerves. *Genes Dev* 1719:2450–2464.
11. Camargo N, Smit AB, Verheijen MH (2009) SREBPs: SREBP function in glia-neuron interactions. *FEBS J* 2763:628–636.
12. de Preux AS, et al. (2007) SREBP-1c expression in Schwann cells is affected by diabetes and nutritional status. *Mol Cell Neurosci* 354:525–534.
13. Shimano H (2002) Sterol regulatory element-binding protein family as global regulators of lipid synthetic genes in energy metabolism. *Vitam Horm* 65:167–194.
14. Matsuda M, et al. (2001) SREBP cleavage-activating protein (SCAP) is required for increased lipid synthesis in liver induced by cholesterol deprivation and insulin elevation. *Genes Dev* 1510:1206–1216.
15. Feltri ML, et al. (1999) P0-Cre transgenic mice for inactivation of adhesion molecules in Schwann cells. *Ann N Y Acad Sci* 883:116–123.
16. Brockes JP, Fields KL, Raff MC (1979) Studies on cultured rat Schwann cells. I. Establishment of purified populations from cultures of peripheral nerve. *Brain Res* 1651:105–118.
17. Avila RL, et al. (2005) Structure and stability of internodal myelin in mouse models of hereditary neuropathy. *J Neuropathol Exp Neurol* 6411:976–990.
18. Wrabetz L, et al. (2006) Different intracellular pathomechanisms produce diverse myelin protein zero neuropathies in transgenic mice. *J Neurosci* 268:2358–2368.
19. Levine YK, Wilkins MH (1971) Structure of oriented lipid bilayers. *Nat New Biol* 23011:69–72.
20. Inouye H, Karthigasan J, Kirschner DA (1989) Membrane structure in isolated and intact myelins. *Biophys J* 561:129–137.
21. Spaar A, Salditt T (2003) Short range order of hydrocarbon chains in fluid phospholipid bilayers studied by X-ray diffraction from highly oriented membranes. *Biophys J* 853:1576–1584.
22. Guzzetta F, Ferriere G, Lyon G (1982) Congenital hypomyelination polyneuropathy. Pathological findings compared with polyneuropathies starting later in life. *Brain* 105Pt 2:395–416.
23. Jurevics H, Bouldin TW, Toews AD, Morell P (1998) Regenerating sciatic nerve does not utilize circulating cholesterol. *Neurochem Res* 233:401–406.
24. Yao JK, Holman RT, Lubozynski MF, Dyck PJ (1980) Changes in fatty acid composition of peripheral nerve myelin in essential fatty acid deficiency. *Arch Biochem Biophys* 2041:175–180.
25. Bourre JM, Youyou A, Durand G, Pascal G (1987) Slow recovery of the fatty acid composition of sciatic nerve in rats fed a diet initially low in n-3 fatty acids. *Lipids* 227:535–538.
26. Lee AG (2003) Lipid-protein interactions in biological membranes: A structural perspective. *Biochim Biophys Acta* 16121:1–40.
27. Horrobin DF (1997) Essential fatty acids in the management of impaired nerve function in diabetes. *Diabetes* 46:S90–93.
28. Chattopadhyay J, Thompson EW, Schmid HH (1992) Nonesterified fatty acids in normal and diabetic rat sciatic nerve. *Lipids* 277:513–517.
29. Norton WT, Poduslo SE (1973) Myelination in rat brain: Method of myelin isolation. *J Neurochem* 214:749–757.
30. Retra K, et al. (2008) A simple and universal method for the separation and identification of phospholipid molecular species. *Rapid Commun Mass Spectrom* 2212:1853–1862.
31. Brugger B, Erben G, Sandhoff R, Wieland FT, Lehmann WD (1997) Quantitative analysis of biological membrane lipids at the low picomole level by nano-electrospray ionization tandem mass spectrometry. *Proc Natl Acad Sci USA* 946:2339–2344.
32. Nadra K, et al. (2008) Phosphatidic acid mediates demyelination in Lpin1 mutant mice. *Genes Dev* 2212:1647–1661.